

# Molecular Dynamics Simulation Study of Parallel Telomeric DNA Quadruplex at Different Ionic Strengths. Evaluation of Water and Ion Models.

## Supporting Information

Matúš Rebič,<sup>\*,†,‡,¶,§</sup> Aatto Laaksonen,<sup>†,¶,||,⊥</sup> Jiří Šponer,<sup>#,®</sup> Jozef Uličný,<sup>§,‡</sup> and  
Francesca Mocci<sup>\*,⊥,†,¶</sup>

E-mail: matus.rebic@mmk.su.se; fmocci@unica.it

Phone: +39 070 675 4390. Fax: +39 070 675 4388

---

\*To whom correspondence should be addressed

<sup>†</sup>Division of Physical Chemistry, Department of Materials and Environmental Chemistry, Arrhenius Laboratory, Stockholm University, 10691 Stockholm, Sweden

<sup>‡</sup>Department of Biophysics, Faculty of Science, P. J. Šafárik University, Jesenná 5, 041 54 Košice, Slovakia

<sup>¶</sup>Science for Life Laboratory (SciLifelab), 17121 Solna, Sweden

<sup>§</sup>Centre for Multimodal Imaging (CMI), Faculty of Science, P. J. Šafárik University, Jesenná 5, 041 54 Košice, Slovakia

<sup>||</sup>Stellenbosch Institute of Advanced Study (STIAS), Wallenberg Research Centre at Stellenbosch University, 7600 Stellenbosch, South Africa

<sup>⊥</sup>Department of Chemical and Geological Sciences, University of Cagliari, I-09042 Monserrato, Italy

<sup>#</sup>Institute of Biophysics, Academy of Sciences of the Czech Republic (AVČR), Kralovopolska 135, 612 65 Brno, Czech Republic

<sup>®</sup>Central European Institute of Technology (CEITEC), Campus Bohunice, Kamenice 5, 625 00 Brno, Czech Republic

## Table of Contents.

|                  | Page  |
|------------------|---|
| <i>Figure S1</i> | RMSF for different Sets S3  |
| <i>Figure S2</i> | RMSD of loop 1, 2 and 3, for different simulation Sets S3             |
| <i>Table S1</i>  | RMSD average for different Sets S3                                    |
| <i>Figure S3</i> | RMSD for different Sets (second run) S4                               |
| <i>Table S2</i>  | RMSD average for different Sets (second run) S4                       |
| <i>Figure S4</i> | RMSF for different Sets (second run) S4                               |
| <i>Figure S5</i> | RMSD for Set 2 of loops 1, 2 and 3 at different KCl concentrations S5 |
| <i>Table S3</i>  | Loops average RMSD for Set 2 at different KCl concentrations S5       |
| <i>Figure S6</i> | RMSD for Set 3 of loops 1, 2 and 3 at different KCl concentrations S6 |
| <i>Table S4</i>  | Loops average RMSD for Set 3 at different KCl concentrations S6       |
| <i>Figure S7</i> | SDF side view, Set 2, 100 mM S7                                       |
| <i>Figure S8</i> | SDF side view, Set 3, 50 mM S7  |
|                  | Mechanism of ion exchange for Set 1 S8-S11                            |

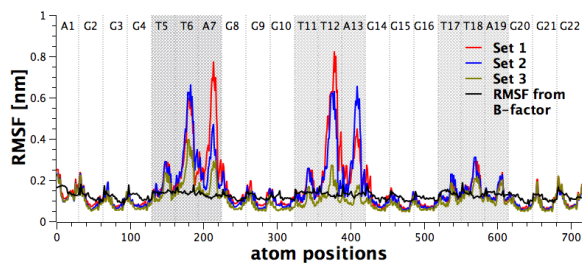


Figure S1: Root mean square fluctuations of atomic positions from the reference experimental 1KF1 crystal structure for different parameter sets. The first simulation.

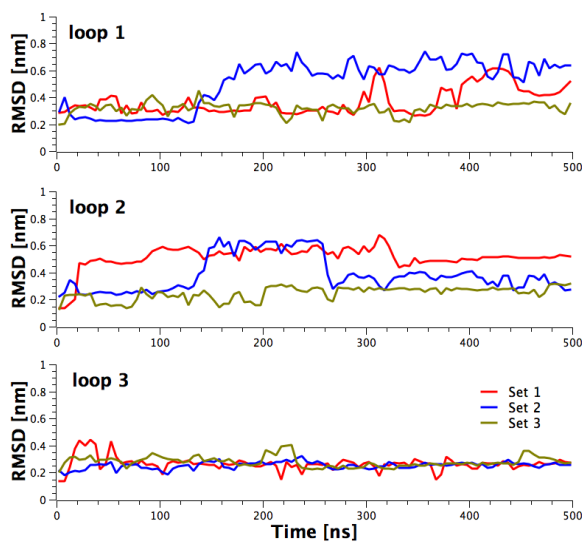


Figure S2: Root mean square deviation of loop 1, 2 and 3, obtained with Sets 1, 2 and 3. The first simulation.

Table S1: Average RMSD and standard deviation (*nm*) of the loops, calculated from the first run of simulations produced with Sets 1, 2 and 3.

| RMSD   | Set 1           | Set 2           | Set 3           |
|--------|-----------------|-----------------|-----------------|
| loop 1 | $0.40 \pm 0.13$ | $0.63 \pm 0.08$ | $0.32 \pm 0.06$ |
| loop 2 | $0.53 \pm 0.07$ | $0.40 \pm 0.12$ | $0.28 \pm 0.04$ |
| loop 3 | $0.26 \pm 0.05$ | $0.26 \pm 0.04$ | $0.27 \pm 0.05$ |

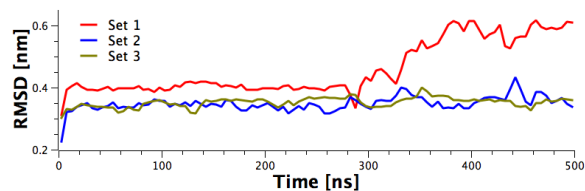


Figure S3: Root mean square deviation of all atom positions from the experimental 1KF1 crystal structure for different parameter sets. The second simulation.

Table S2: Average RMSD and standard deviation ( $nm$ ), from the second run of simulations produced with Sets 1, 2 and 3.

| RMSD  | average ( $nm$ ) | $\sigma$ ( $nm$ ) |
|-------|------------------|-------------------|
| Set 1 | 0.500            | $\pm 0.090$       |
| Set 2 | 0.362            | $\pm 0.029$       |
| Set 3 | 0.357            | $\pm 0.019$       |

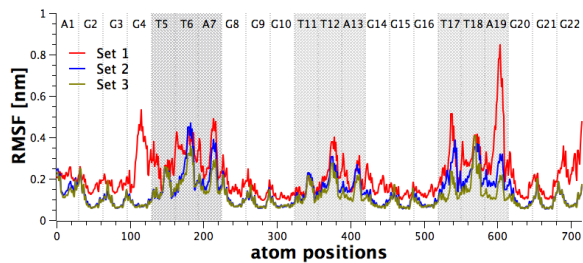


Figure S4: Root mean square fluctuations of atomic positions from the reference experimental 1KF1 crystal structure for different parameter sets. The second simulation.

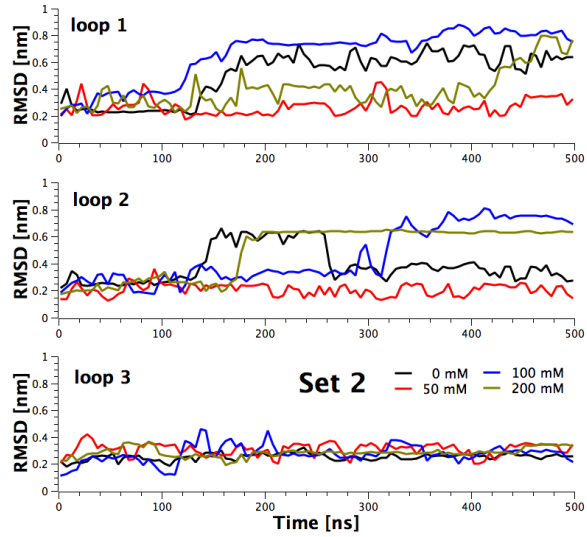


Figure S5: Root mean square deviation for Set 2 of loops 1, 2 and 3 at different KCl concentrations.

Table S3: Average RMSD and standard deviation ( $nm$ ), of the loops in Set 2 simulations with different KCl concentrations.

| RMSD   | 0 mM            | 50 mM           | 100 mM          | 200 mM          |
|--------|-----------------|-----------------|-----------------|-----------------|
| loop 1 | $0.63 \pm 0.08$ | $0.28 \pm 0.08$ | $0.78 \pm 0.07$ | $0.45 \pm 0.16$ |
| loop 2 | $0.40 \pm 0.12$ | $0.20 \pm 0.06$ | $0.58 \pm 0.20$ | $0.64 \pm 0.02$ |
| loop 3 | $0.26 \pm 0.04$ | $0.31 \pm 0.07$ | $0.29 \pm 0.06$ | $0.29 \pm 0.04$ |

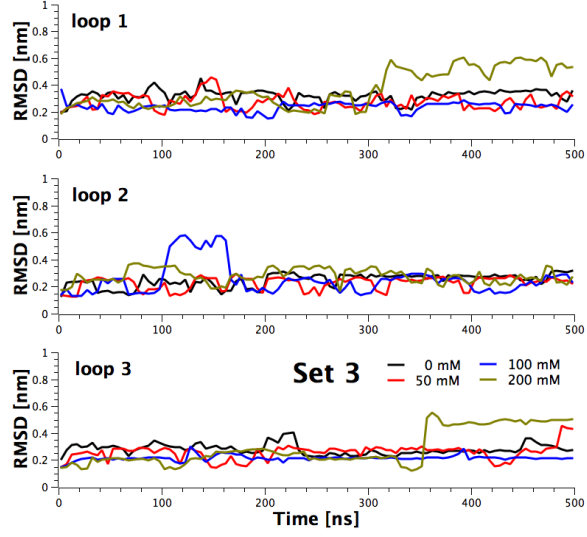


Figure S6: Root mean square deviation for Set 3 of loops 1, 2 and 3 at different KCl concentrations.

Table S4: Average RMSD and standard deviation ( $nm$ ), of the loops in Set 3 simulations with different KCl concentrations.

| RMSD   | 0 mM            | 50 mM           | 100 mM          | 200 mM          |
|--------|-----------------|-----------------|-----------------|-----------------|
| loop 1 | $0.32 \pm 0.06$ | $0.27 \pm 0.07$ | $0.24 \pm 0.05$ | $0.43 \pm 0.15$ |
| loop 2 | $0.28 \pm 0.04$ | $0.24 \pm 0.05$ | $0.23 \pm 0.06$ | $0.28 \pm 0.07$ |
| loop 3 | $0.27 \pm 0.06$ | $0.27 \pm 0.07$ | $0.22 \pm 0.03$ | $0.35 \pm 0.14$ |

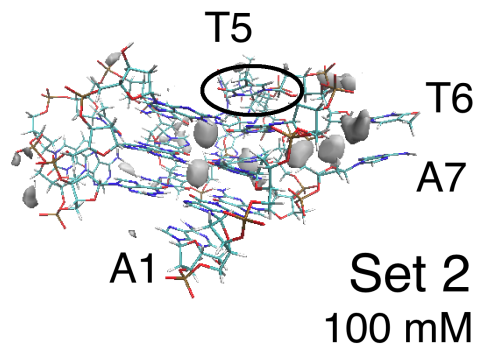


Figure S7: Side view of spatial distribution functions for potassium around averaged quadruplex structure at 100 *mM* KCl concentration for Set 2. Isodensity surface normalized value: 300.

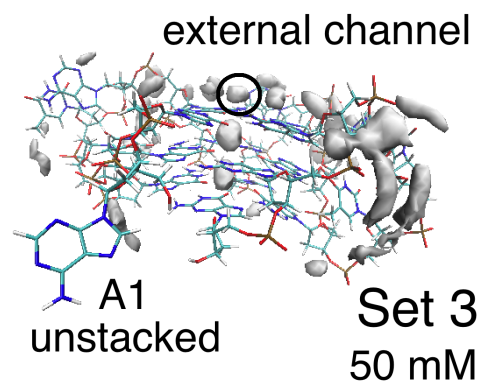


Figure S8: Side view of spatial distribution functions for potassium around averaged quadruplex structure at 50 *mM* KCl concentration for Set 3. Isodensity surface normalized value: 300.

# Mechanism of ion exchange

At the beginning of the simulation two ions were coordinated inside the channel, as shown in Figure S9.

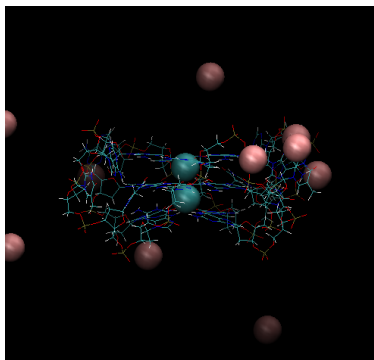


Figure S9: Ions in the channel (cyano) at the beginning of the simulation. The external Potassium ions are represented in pink.

The trajectory of the distance between the ions placed in the channel at the beginning of the simulation is shown in Figure S10, together with the distance between the ion that remains in the channel during the entire simulation, and the ion which enters in the channel after one ion exits. In the following we describe the mechanism of the exchange by using the snapshots of key moments of the exchange.

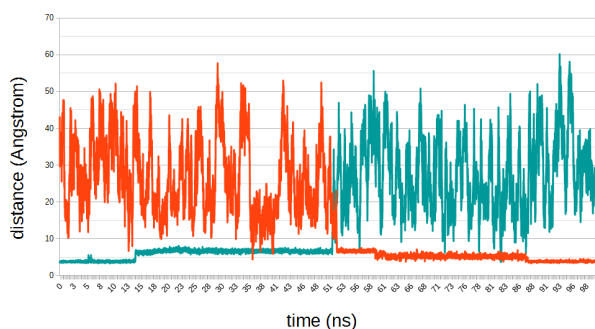


Figure S10: Distances between channel ions. Cyano and Orange lines represent the distances between the ions involved in the exchange and the ion that remains in the channel.

At about 15 ns one of the ions leaves the inner part of the channel, and coordinates at the external rim, see Figure S11, interacting with the adenine base A1 and with several water

molecules. Such a coordination, is kept for more than 30 ns, and frequent water exchange is observed in the ion solvating shell.

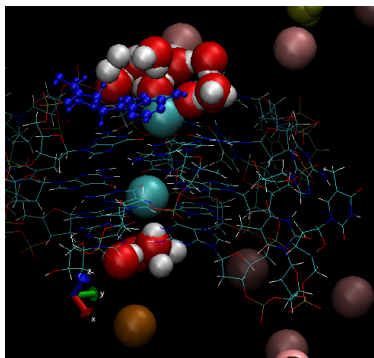


Figure S11: Typical coordination around the Potassium ion positioned at the external rim of the channel (top of the figure). A1 base is represented in blue.

The substitution of the ion at the channel's rim by one solvating water molecules triggers the ion departure from the rim of the channel, as shown in Figure S12. For visual guidance the water molecules which swaps with the ion is colored in magenta. A second water molecule, in yellow, soon swaps with the violet one.

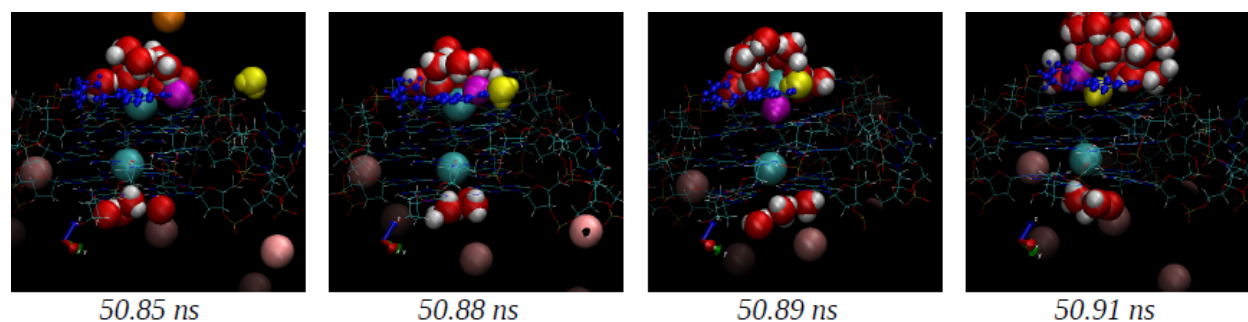


Figure S12: Exchange between the Potassium ion at the external rim of the channel with one of the ion solvating water molecule (in violet). Soon after (50.91 ns) the water molecule in violet exchange with another one, in yellow in the picture.

As shown in Figure S13 the water molecule spends some time at the rim of the channel before being exchanged with another one, and the water exchange continues until a water

molecules moves from the rim to the inner part of the channel; the entrance seems to be triggered by an ion coming close to the entrance (51.40 -51.44 ns).

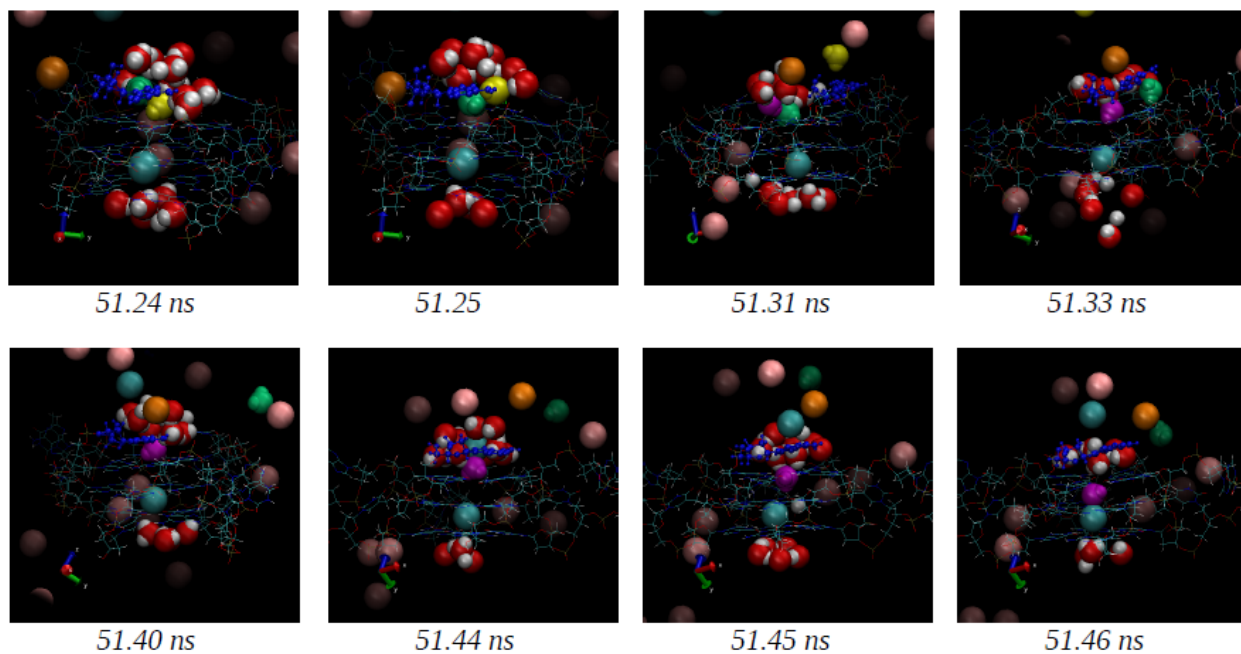


Figure S13: Exchange between water molecules at the external rim of the channel. At 51.40 a water molecule eventually enters in the channel.

Soon after the water molecule enters the channel, one ion coordinates to the rim of the channel, and remains stable for some time, see Figure S14.

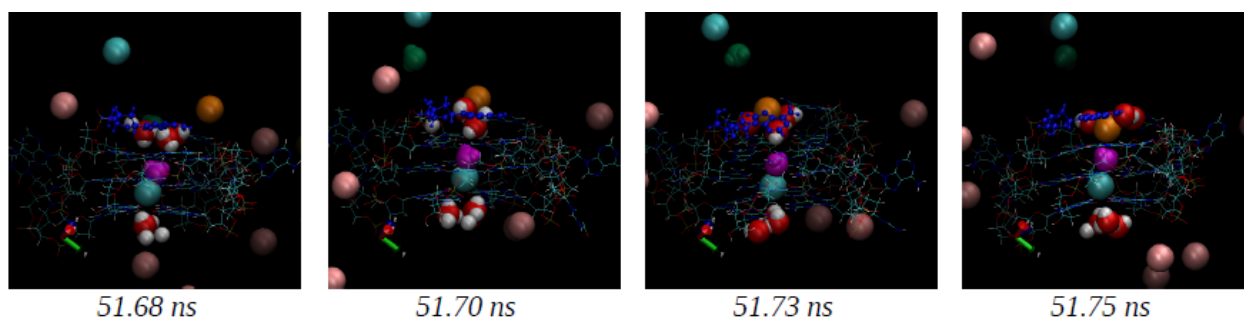


Figure S14: Exchange between water molecules at the external rim of the channel. At 51.40 a water molecule eventually enters in the channel.

The magenta water molecule remains in the channel for about 8 ns. After it leaves the channel, the ion which was coordinated at the external part of the rim, repeatedly enters

and leaves the channel up to around 88 ns. During this period (59-88 ns) the top G-tetrad is highly deformed and two of the guanine bases are not connected through H-bonds because one water molecule is placed between the two, coordinating also the Potassium ion, see Figure S15. After 88.5 ns, after the water molecule between the guanine bases moves to the bulk without being replaced by any other water molecule, the top G-tetrad fully recovers the 8 hydrogen bonds between the guanine bases, and the Orange ion remains inside the channel for the remaining of the simulation.

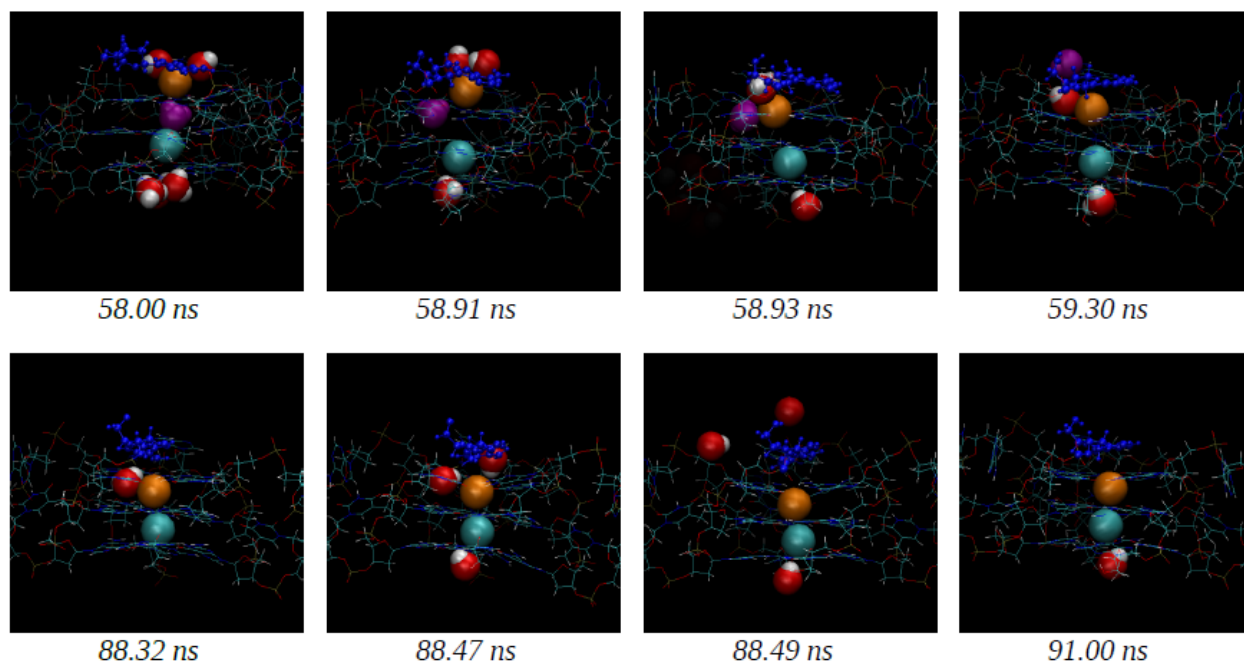


Figure S15: Exit of the violet water molecule from the channel. the exiting water molecules coordinates with the ion in the rim of the channel, and with two guanine bases (58.00-58.93 ns). At 59.30 another water molecule exchanges with the violet water molecule, and replaces it. The water exchange continues until 88.47 ns, when a water molecule exits without being replaced and the ion eventually enter in the channel.